Imidazole-Catalyzed Displacement of an Amine from an Amide by a Neighboring Hydroxyl Group. A Model for the Acylation of Chymotrypsin[1,2]

C. J. Belke, S. C. K. Su, and J. A. Shafer*

Contribution from the Department of Biological Chemistry, The University of Michigan, Ann Arbor, Michigan 48104.
Received October 1, 1970

Abstract: Acids and bases catalyze lactonization (to phthalide) of 2-hydroxymethylbenzamide (**1a**) and *N*-benzyl-2-hydroxymethylbenzamide (**1b**). Kinetic evidence indicates that lactonization of these amides is a multistep process with a change in rate-controlling step occurring at pH ~8. The dependence of catalytic efficiency of bases on the pK_a of the conjugate acid of the catalyst suggests that below pH ~8 the rate-determining step for base-catalyzed lactonization of **1a** involves diffusion-controlled proton transfer between catalyst and tetrahedral intermediates. Imidazole is an efficient catalyst for lactonization of **1a** and **1b**. At 25°, the apparent second-order rate constant for imidazole-catalyzed lactonization of **1a** is 4.5×10^{-3} min^{-1} M^{-1}. The imidazole-catalyzed lactonization of **1a** is the first model system which can account for the rapid rates of acylation of chymotrypsin by amide substrates in terms of an imidazole-facilitated attack of a hydroxyl group on an amide. The acylation of chymotrypsin by amide substrates is the rate-determining step in chymotrypsin-catalyzed hydrolysis of amides. This reaction also involves attack of a hydroxyl group (of Ser-195), which is facilitated by an imidazole group (of His-57).

An imidazole group of a histidyl residue and a hydroxyl group of a seryl residue have been implicated in the catalytic activity of serine proteinases.[3] For example, direct evidence has been presented for the involvement of Ser-195[4] and His-57[5] in the catalytic activity of α-chymotrypsin. The imidazole group of His-57 is thought to facilitate attack by the hydroxyl group of Ser-195 on amide substrates. Consequently, an amine is displaced from the amide substrate and an acyl–enzyme intermediate is formed in which the active seryl residue is esterified. The enzyme is then rapidly regenerated on the hydrolysis of this ester whose cleavage is also thought to be catalyzed by His-57.

Because hydroxyamides are capable of undergoing analogous acylation and deacylation reactions, they have been studied in several laboratories as models for the enzyme–substrate complex.[6] An important test of our understanding of the mechanism by which serine proteinases catalyze hydrolytic reactions involves demonstrating that imidazole can indeed facilitate displacement of an amine from an amide by a hydroxyl group. Although neighboring hydroxyl groups have been reported to facilitate the hydrolysis of hydroxyamides (*e.g.*, hydroxybutyramide[6b] and hydroxybutyranilide[6c]), reports of imidazole-catalyzed lactonization of hydroxyamides are conspicuous by their absence. The imidazole-catalyzed lactonization of amides **1a** and **1b** reported here demonstrates, for the first time, the feasibility of an imidazole-facilitated attack of a hydroxyl group on an amido group, and provides us with a model for the acylation of a serine proteinase by its substrate.

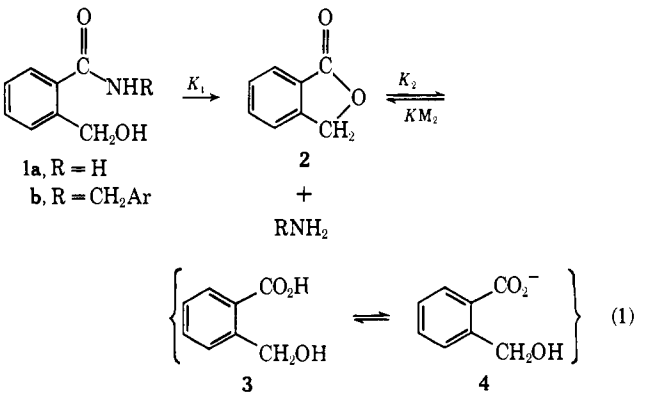

Experimental Section

Materials. Phthalide was obtained from Matheson Coleman and Bell and recrystallized from water before use; mp 73–74° corrected (lit.[7] mp 73°).

N-Benzyl-2-hydroxymethylbenzamide was prepared by stirring 5 g (0.037 mol) of phthalide with 50 g (0.47 mol) of benzylamine for 6 hr at room temperature. The crude product oiled out of the reaction mixture upon addition of 200 ml of petroleum ether. After repeated cooling and stirring, the oil solidified. The solid

(1) This study was supported in part by a grant (AM-09276) from the National Institutes of Health, U. S. Public Health Service.

(2) (a) A preliminary announcement of this work was made at the 158th National Meeting of the American Chemical Society, New York, N. Y., Sept 1969. (b) Part of this work is described in a Ph.D. Dissertation to be submitted by C. J. Belke to the Graduate School of The University of Michigan.

(3) For a comprehensive discussion of evidence implicating these residues in the catalytic activity of serine proteinases see M. L. Bender and F. J. Kézdy, *Annu. Rev. Biochem.*, **34**, 49 (1965).

(4) (a) R. A. Oosterbaan and M. E. van Adrichem, *Biochem. Biophys. Acta*, 27, 423 (1958); (b) A. M. Gold, *Biochemistry*, **4**, 897 (1965); (c) Y. Shalitin and J. R. Brown, *Biochem. Biophys. Res. Commun.*, **24**, 817 (1966); (d) D. C. Shaw, W. H. Stein, and S. Moore, *J. Biol. Chem.*, **239**, PC671 (1964); (f) H. Weiner, W. N. White, D. G. Hoare, and D. E. Koshland, Jr., *J. Amer. Chem. Soc.*, **88**, 3851 (1966).

(5) (a) G. Schoellmann and E. Shaw, *Biochemistry*, 2, 252 (1963); (b) L. B. Smillie and B. S. Hartley, *Biochem. J.*, **101**, 232 (1966); (c) K. J. Stevenson and L. B. Smillie, *J. Mol. Biol.*, **12**, 937 (1965); (d) H. J. Schramm, *Biochem. Z.*, **342**, 139 (1965); (e) Y. Nakagawa and M. L. Bender, *J. Amer. Chem. Soc.*, **91**, 1566 (1969).

(6) (a) For examples of neighboring hydroxyl group participation in the hydrolysis of amides see T. C. Bruice and S. J. Benkovic, "Bioorganic Mechanisms," Vol. 1, W. A. Benjamin, New York, N. Y., 1966, pp 146–166; (b) T. C. Bruice and F. H. Marquardt, *J. Amer. Chem. Soc.*, **84**, 365 (1962); (c) B. A. Cunningham and G. L. Schmir, *ibid.*, **89**, 917 (1967).

(7) J. Hessert, *Ber.*, 10, 1445 (1877).

was recrystallized three times from ethyl acetate; mp 134–135° corrected.

Anal. Calcd for $C_{15}H_{15}NO_2$: C, 74.67; H, 6.27; N, 5.80. Found: C, 74.52; H, 6.32; N, 5.69.

2-Hydroxymethylbenzamide was prepared by adding 25 ml (~1 mol) of liquid ammonia to 5 g (0.037 mol) of phthalide in 50 ml of tetrahydrofuran in a 100-ml stainless steel reaction tube made by the Parr Instrument Co. After keeping the sealed reaction tube at 60° for 72 hr, tetrahydrofuran and ammonia were removed from the reaction mixture under reduced pressure on a rotary evaporator. The remaining solid was extracted with carbon tetrachloride to remove any unreacted phthalide and then recrystallized three times from chloroform; mp 148–149° corrected.

Anal. Calcd for $C_8H_9NO_2$: C, 63.56; H, 6.00; N, 9.26. Found: C, 63.55; H, 6.09; N, 9.22.

Imidazole obtained from the Aldrich Chemical Co. was recrystallized three times from benzene and sublimed under reduced pressure; mp 88–89° corrected (lit.[8] mp 90.2–90.6°). Triethylamine (from Eastman Organic Chemicals) was treated with phenylisocyanate and redistilled. Triethylamine hydrochloride was prepared by slowly neutralizing a cold aqueous solution of triethylamine with cold concentrated hydrochloric acid. The water was removed under reduced pressure on a rotary evaporator and the remaining triethylamine hydrochloride was recrystallized from absolute ethanol.

Chloroacetic acid (from Eastman Organic Chemicals) was recrystallized from water.

Methoxyacetic acid (from Eastman Organic Chemicals) was distilled under reduced pressure.

The distilled water supplied to the laboratory was run through a demineralizer and redistilled in an all-glass still. All other chemicals used were Mallinckrodt, Fisher, or Baker-Adamson analytical reagents.

Methods. Measurements of pH were made using a Radiometer Model 4B pH meter which was standardized with a 1:1 phosphate–NBS primary standard solution.[9] The response of the glass electrode was determined with NBS primary standard solutions (borax and phthalate). The glass electrode response (pH meter reading) was essentially a linear function of the pH between 4 and 9. Measurements of pH were made before and after each kinetic run, and the average value of pH was used. The total change in pH during a kinetic run in a buffered solution rarely exceeded 0.02 unit.

Hydrogen ion concentrations were estimated from the pH and the mean activity coefficient of hydrogen chloride in potassium chloride solutions. The mean activity coefficients used (0.70 at 40° and 0.68 at 60° with $\Gamma/2 = 0.822$ *M*) were interpolated from the data listed by Harned and Owen.[10] The hydroxide ion concentration was estimated from the hydrogen ion concentration and the formal dissociation constant for water (K_w'), *i.e.*, $K_w\alpha_{H_2O}/\gamma_{H^+}\gamma_{OH^-}$ which was interpolated from the data listed in ref 10. The formal dissociation constants used were 5.2×10^{-14} *M* at 40° and 1.81×10^{-13} *M* at 60° with $\Gamma/2 = 0.822$ *M*.[11]

Rate Measurements. Reaction 1 was followed spectrophotometrically by observing the build up and decay of absorbance (at 275 nm) corresponding to the formation and hydrolysis of phthalide. Reactions were carried out in buffered solution with $\Gamma/2 = 0.822$ *M* (maintained with KCl) and containing 3.2% ethanol or 3.2% acetonitrile. Replacing ethanol with acetonitrile did not detectably alter any rate constants. Reactions were initiated by adding 1 part of a solution of reactant in ethanol or acetonitrile to 30 parts of an aqueous solution of buffer which was previously brought to the reaction temperature. The reaction mixture was contained in either a glass-stoppered cuvette or volumetric flask. When the reaction was carried out in a cuvette, the absorbance was monitored continuously with a Gilford 2000 multiple sample absorbance recorder. Constant temperature (±0.1°) was maintained by circulating water from a thermostated bath through thermospacers surrounding the cell compartment. When the reaction was carried out in a volumetric flask, aliquots of the reaction mixture were removed at appropriate times and rapidly cooled to room temperature, and their absorbancies were determined. The reaction mixture was maintained at constant temperature (±0.1°) by keeping the volumetric flask in an oil bath. Temperatures of reaction solutions were measured with an NBS certified thermometer.

Rate constants were usually obtained by fitting the observed time dependence of absorbance to eq 2. A computer program was designed to select the values of K_1, K_2, and KM_2 which gave the minimum deviation from eq 2.

$$\frac{D - D_f}{D_{2f} - D_f} = \frac{K_1}{K_1 - K_2 - KM_2} \times \left[\exp(-K_2 t - KM_2 t) - \left(1 - \frac{KM_2}{K_1}\right)\left(\frac{D_{2f} - D_{3f}}{D_{2f} - D_f}\right) \times \exp(-K_1 t)\right] + \frac{D_i - D_{3f}}{D_{2f} - D_f} \exp(-K_1 t) \quad (2)$$

The subscripts i and f in eq 2 denote initial and final absorbancies. D represents the absorbance at time t. D_{2f} is the value of the final absorbance when no hydrolysis of phthalide occurs. D_{3f} is the value of the final absorbance when the hydrolysis of phthalide goes to completion. For hydrolysis of 8.26×10^{-4} *M* amide **1a** at 40°, $D_i = 0.390$, $D_{2f} = 1.475$, and $D_{3f} = 0.345$.

The products of reaction of **1a** and **1b** were characterized by the identity of the ultraviolet spectra taken at the end of kinetic runs with that of *o*-hydroxymethylbenzoate plus amine. Under conditions in which the hydrolysis of phthalide did not go to completion, the final spectrum could be quantitatively rationalized in terms of a mixture of *o*-hydroxymethylbenzoate, phthalide, and amine.

The hydrolysis of phthalide (**2**) was also studied separately, and K_2 and KM_2 were evaluated from the first-order approach of the concentration of phthalide (**2**) to its equilibrium value and the fraction of phthalide present at equilibrium. Studies of the hydrolysis of **1** (to **3** and **4**) and the separate hydrolysis of **2** (to **3** and **4**) lead to essentially the same values for K_2 and KM_2.

Below pH 6, hydrolysis of phthalide is not observed and cyclization of **1** is a first-order process described by eq 3. Values of K_1

$$-\ln(D_f - D) = K_1 t - \ln(D_f - D_i) \quad (3)$$

were obtained from slopes of linear plots of $-\ln(D_f - D)$ *vs.* time.

Results

Buffers increase the rate of cyclization of hydroxybenzamides **1a** and **1b**. K_1 is a linear function of the total buffer concentration, [Bt] at a fixed buffer ratio (eq 4). K_{1B_t} is the apparent second-order rate constant for

$$K_1 = K_{1_0} + K_{1B_t}[\mathrm{Bt}] \quad (4)$$

buffer-catalyzed formation of phthalide and K_{1_0} is the rate constant for the formation of phthalide in the absence of buffer.

Both the acidic and basic components of the buffer catalyze formation of phthalide. Figure 1 depicts the effect of imidazole on the apparent rate constant for cyclization of amides **1a** and **1b**. Clearly, imidazole is more efficient in catalyzing cyclization of the hydroxyamides than imidazolium ion. Acids with a $pK_a < 5$, however, are more efficient than their conjugate bases in catalyzing cyclization. Unless otherwise specified, in most cases K_{1B_t} is a linear function (eq 5) of the fraction of basic component in the buffer (f) (Figure 2)

$$K_{1B_t} = K_{1_a}(1 - f) + K_{1_b} f \quad (5)$$

where K_{1_a} and K_{1_b} are apparent second-order rate constants for catalysis of cyclization by the acidic and basic components of the buffer. K_{1_a} and K_{1_b} were determined by extrapolating the linear plots of K_{1B_t} *vs.* f to $f = 0$ and $f = 1$.

(8) F. Cramer, *Angew. Chem.*, 72, 236 (1960).

(9) R. G. Bates, "Determination of pH Theory & Practice," Wiley, New York, N. Y., 1964, pp 62–94, 123–130.

(10) H. S. Harned and B. B. Owen, "The Physical Chemistry of Electrolytic Solutions," 3rd ed, Reinhold, New York, N. Y., 1958, pp 638, 748, and 752.

(11) The effects of 3.2% acetonitrile or ethanol on the activity coefficients, the formal dissociation constant of water, and the pH measurement were neglected. Undoubtedly, these effects introduce a small systematic error into the absolute magnitude of the second-order rate constants reported in this work.

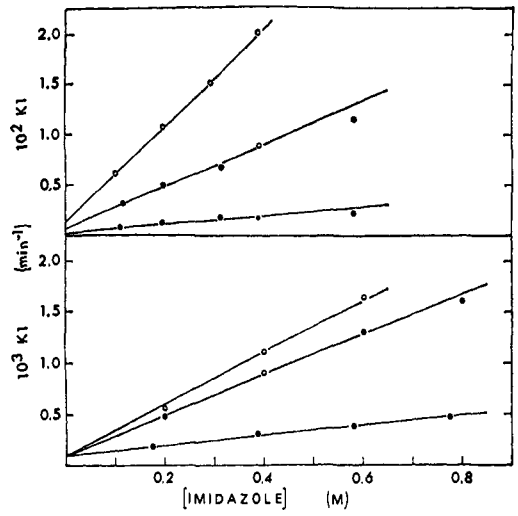

Figure 1. Dependence of the pseudo-first-order rate constant (K_1) for lactonization of **1a** at 60° (top) and **1b** at 60° (bottom) on the total concentration of imidazole buffer: ○, [IM]/[IMH$^+$] = 9; ◐ [IM]/[IMH$^+$] = 1; ●, [IM]/[IMH$^+$] = 1/9.

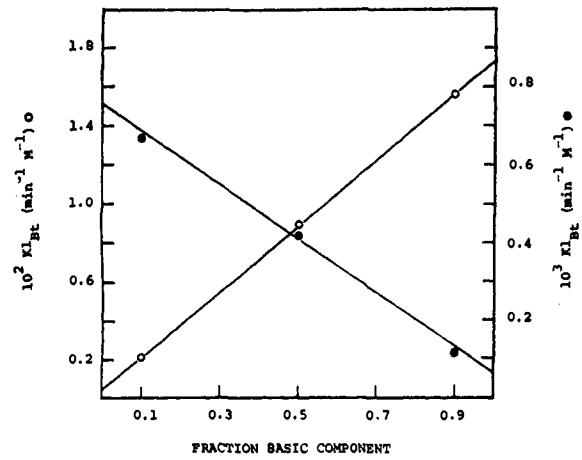

Figure 2. Dependence of the apparent second-order rate constant (K_{1Bt}) for buffer-catalyzed lactonization of **1a** at 40° on the fraction of basic component in the buffer: ○, IM–IMH$^+$ buffers, left ordinate; ●, acetic acid–acetate buffers, right ordinate.

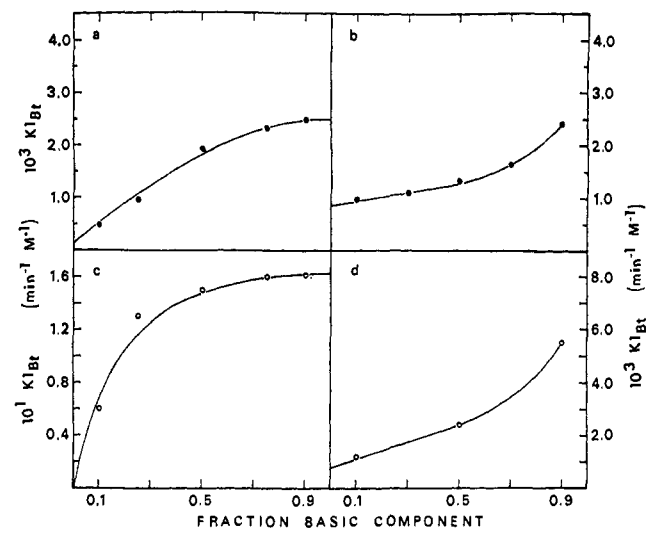

Figure 3. Dependence of the apparent second-order rate constant (K_{1Bt}) for buffer-catalyzed lactonization of **1b** at 60° (●) and **1a** at 40° (○) on the fraction basic component in the buffer: curve a, IM–IMH$^+$ buffers, solid line calculated using eq 12; curve b, $H_2PO_4^-$–HPO_4^{2-} buffers; curve c, HCO_3^-–CO_3^{2-} buffers, solid line calculated using eq 13; curve d, $H_2PO_4^-$–HPO_4^{2-} buffers, solid line calculated using eq 16.

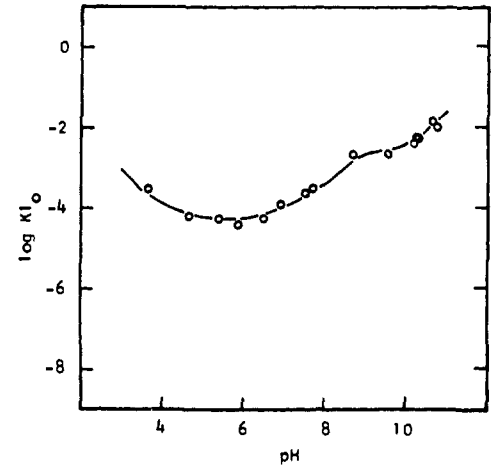

Figure 4. Dependence of the pseudo-first-order rate constant (K_{1_0}) on pH for lactonization of **1a** at 40° in the absence of buffer. Solid line calculated using eq 15.

Equation 5, however, does not represent the dependence of K_{1B_i} on f for the imidazole- and phosphate-catalyzed cyclization of amide **1b** and the carbonate- and phosphate-catalyzed cyclization of amide **1a** (Figure 3). This result is rationalized in terms of a change in rate-determining step as f is increased (see Discussion).

The pH dependence of lactonization of amide **1a** is illustrated in Figure 4. The broad plateaus in the pH–rate profile are a consequence of an efficient (relative to hydroxide ion and hydronium ion catalyzed cyclization) "spontaneous" or water-catalyzed reaction. Water-catalyzed lactonization of γ-hydroxybutyramide is also efficient and probably makes the major contribution to the rate of cyclization of γ-hydroxybutyramide at pH values near neutrality.[6b]

Whereas apparent rate constants (in the absence of buffer) for many acid–base-catalyzed reactions are simple linear functions of the hydronium ion and hydroxide ion concentration (eq 6), eq 6 does not describe the dependence of K_{1_0} for cyclization of amide **1a** on the hydronium and hydroxide ion concentration (Figure 4). Cunningham and Schmir[6c] observed a similar nonlinear dependence for the rate constant for lactonization of hydroxybutyranilide. These authors interpreted their results in terms of a change in rate-determining step for lactonization.

$$K_{1_0} = K_{1H_2O}[H_2O] + K_{1H_3O}[H_3O^+] + K_{1OH}[OH^-] \quad (6)$$

The effect of acids and bases on the rate of lactonization of **1a** and **1b** has been interpreted in terms of a multistep process with a change in rate-determining step from step A to step B occurring at pH 8–9 (for amide **1a**). The dependence of K_{1_b} (for lactonization of amide **1a**) on the pK_a of the conjugate acid of the catalyst when step A is rate limiting and when step B is rate limiting is depicted in Figures 5 and 6, respectively.

A Brønsted plot for base catalysis of step A exhibits a break around pK_a 7. Below pK_a 7, the slope is close to unity. Bases with pK_a > 7 (CO_3^{2-}, PO_4^{3-}, and OH^-)

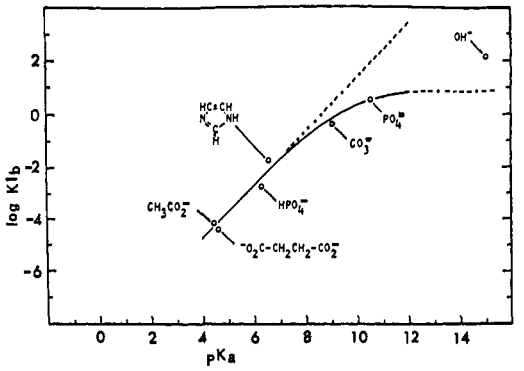

Figure 5. Brønsted plot for base catalysis of step A in the lactonization of **1a** at 40°. pK_a's were calculated from hydrogen ion concentrations in partially neutralized solutions of catalyst at 40°, $\Gamma/2 = 0.822$. The following statistical corrections were applied to observed rate and acid dissociation constants. The observed values for the catalytic efficiencies of $^{-}O_2CCH_2CH_2CO_2^{-}$, HPO_4^{2-}, CO_3^{2-}, and PO_4^{3-} were divided by 2, 2, 2, and 3, respectively. The observed acid dissociation constants of $HO_2CCH_2CH_2CO_2^{-}$, HCO_3^{-}, and HPO_4^{2-} were multiplied by 2, 2, and 3, respectively.

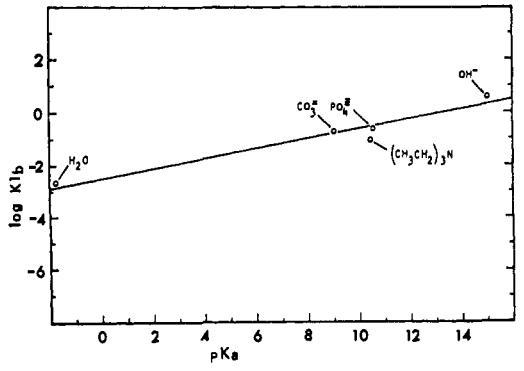

Figure 6. Brønsted plot for base catalysis of step B in the lactonization of **1a** at 40°. See legend to Figure 5 for statistical corrections applied to rate and acid dissociation constants.

deviate markedly from an extension of the line determined below pK_a 7 (Figure 5). Step B appears to be characterized by a Brønsted β value of ~0.2 over a wide range of basicity (Figure 6).

In the pH range 1–8, the dependence of K_{1a} on the pK_a of the acid component of the buffer is described by the Brønsted equation (eq 7) with $\alpha = 0.39$ and $\alpha =$

$$\log K_{1a} = G_A - \alpha pK_a \qquad (7)$$

0.41 for lactonization of amides **1a** and **1b** at 60° (Figure 7).

The temperature dependence of K_{1b} for imidazole-catalyzed lactonization of amides **1a** and **1b** is shown in Figure 8. The linearity of these Arrhenius plots indicates that the activation parameters for steps A and B are not markedly different. K_{1b} for the imidazole-catalyzed lactonization of **1b** was estimated from the value of $K_{1B'}$ obtained for imidazole buffer in which [IM]/[IMH$^+$] = 9 ($f = 0.9$). This value is at least 90% of the true value of K_{1b}, since the slope of plots of $K_{1B'}$ *vs.* f (for amide **1b**) is close to zero near $f = 0.9$ (*e.g.*, Figure 3). K_{1b} for imidazole-catalyzed lactonization of amide **1a** was obtained by extrapolating plots of $K_{1B'}$ *vs.* f to $f = 1.0$ (*e.g.*, Figure 2).

The activation energies for imidazole-catalyzed lactonization of **1a** and **1b** are 14.3 and 15.6 kcal/mol, respectively. Interestingly, the activation energy for imidazole-catalyzed lactonization of **1a** is similar to the value of 14.8 kcal/mol obtained for the activation energy associated with the hydroxide ion catalyzed hydrolysis of benzamide.[12] At 25°, the second-order rate constant for hydroxide ion catalyzed hydrolysis of benzamide is 0.69×10^{-3} min^{-1} M^{-1},[13] whereas the second-order rate constant for imidazole-catalyzed lactonization of **1a** is 4.5×10^{-3} min^{-1} M^{-1}. Thus (in a formal sense) attack by the weak base, imidazole, and a properly oriented un-ionized hydroxyl group can be more efficient in displacing an amine from an amide than direct intermolecular attack by the powerful nucleophile, hydroxide ion. This finding may be pertinent to the mechanism of action of serine proteinases, since under physiological conditions it is easier to increase the local concentration of imidazole than it is to increase the local concentration of hydroxide ion (or alkoxide ion) at the active site of a proteolytic enzyme.

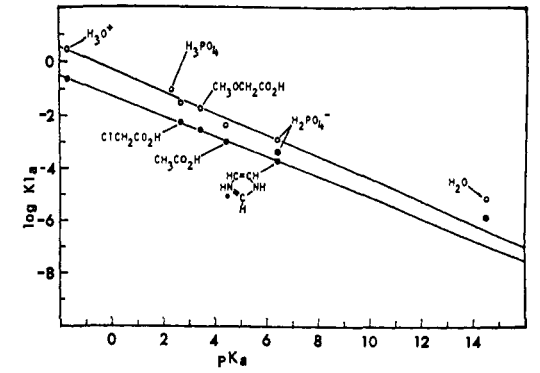

Figure 7. Brønsted plots for acid catalysis of step A in the lactonization of **1a** (○) and **1b** (●) at 60°. pK_a's were calculated from hydrogen ion concentrations in partially neutralized solutions of catalyst at 60°, $\Gamma/2 = 0.822$. The following statistical corrections were applied to observed rate and acid dissociation constants. The observed values for the catalytic efficiencies of H_3PO_4 and $H_2PO_4^{-}$ were divided by 3 and 2, respectively. The observed acid dissociation constant of H_3PO_4 was divided by 3.

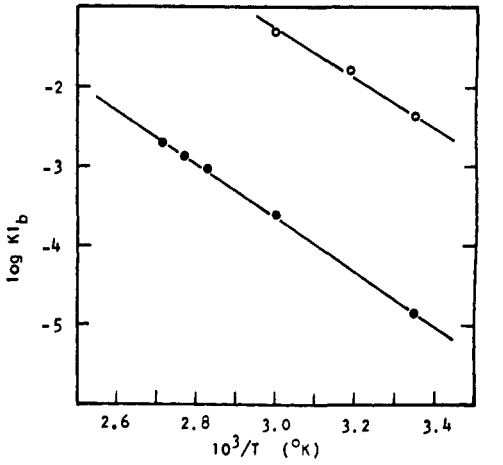

Figure 8. Arrhenius plots for imidazole-catalyzed lactonization of **1a** (○) and **1b** (●).

(12) M. L. Bender, R. D. Ginger, and J. P. Unik, *J. Amer. Chem. Soc.*, **80**, 1044 (1958).

(13) Interpolated from the temperature dependence of rate constants listed in ref 12.

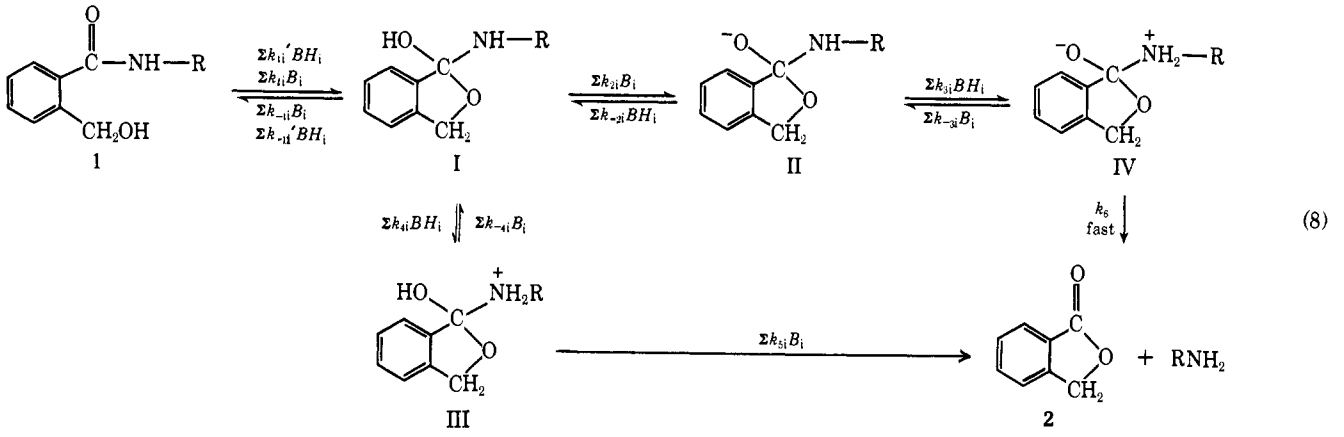

(8)

Discussion

A Possible Mechanism for Lactonization of 2-Hydroxymethylbenzamides. Effects of acids and bases on rates of lactonization of amides **1a** and **1b** can be rationalized in terms of the reaction pathway depicted in eq 8.

Below pH ~8, conversion of I to II and IV *via* diffusion-controlled proton transfer to and from the catalyst is rate determining, and base-catalyzed lactonization with $\beta = 1$ is observed. A β value of unity for base-catalyzed formation of phthalide below pH 8 indicates diffusion-controlled proton transfer is rate determining below pH 8.[14] Acid catalysis of lactonization (below pH ~8) is characterized by a Brønsted α value of less than unity, so that proton transfer is probably concerted with breaking of a covalent bond to carbon. This result suggests that the rate-determining step for the observed acid-catalyzed lactonization involves catalysis of elimination of amine from III by the conjugate base of the catalyst. Above pH 8, cyclization of **1** to I is rate determining. The conversion of **1** to I is subject to general base catalysis, and general base catalysis ($0 < \beta < 1$) of lactonization is observed.

Exclusion of Alternate Pathways. The possibility that imidazole catalyzes cyclization of the hydroxymethylbenzamides by catalyzing diffusion-controlled ionization of the neighboring hydroxyl group can be excluded. The second-order rate constant for this reaction (eq 9) is given by $k_1 = k_{-1}K_1/K_{IMH}$, where K_1 and K_{IMH} represent the acid dissociation constants of the amide substrate and imidazolium ion, respectively.

Since $K_{IMH} \sim 10^{-7}$ and $K_1 > 10^{-16}$, reaction of imidazolium ion with $\mathbf{1}^-$ should be diffusion controlled[14] (*i.e.*, $k_d \sim 10^{10}$ sec$^{-1}M^{-1}$) and k_1 should be greater than 10 sec$^{-1}M^{-1}$. This value for the second-order rate constant for the imidazole-catalyzed ionization of the hydroxyl group in the amide substrates is several orders of magnitude greater than the second-order rate constants observed for imidazole-catalyzed cyclization of amides **1a** and **1b**. Thus, below pH 8, base-catalyzed formation of phthalide must involve diffusion-controlled proton transfer to or from an intermediate, in the rate-determining step. Examples of rate-determining diffusion-controlled proton transfer involving intermediates in the thiazoline hydrolysis have been presented by Barnett and Jencks[15] and intermediates in thioimidate hydrolysis by Chaturvedi and Schmir.[16]

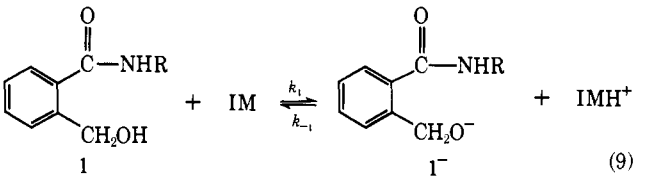

(9)

Reaction pathways involving conversion of II directly to products can be excluded. A multistep pathway in which formation of II from **1** is rate determining, with a rapid unimolecular decomposition of II to phthalide, is unlikely. Elimination of alkoxide ion from the tetrahedral carbon atom in II should be more facile than elimination of RNH^-, so that $\mathbf{1}^-$ (and therefore **1**) would be in equilibrium with II, and the rate of formation of II could not be rate determining. If, at pH values above 8, conversion of II directly to products (*via* transition state V) were rate determining, this reaction would be consistent with the observation that $0 < \beta < 1$ above pH 8. The step characterized by

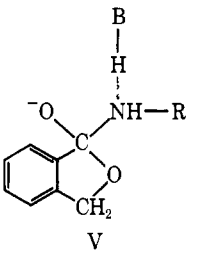

V

$\beta = 1$ would then be conversion of I to II. When $\beta = 1$ (below pH ~8), conversion of I to II would be rate determining and reaction of II with BH to form I would be diffusion controlled. For conversion of I to II to be rate determining, reaction of II with BH to form phthalide must be faster than a diffusion-controlled reaction. However, reaction of II with BH to form phthalide involves breaking of a C–N bond in addition to the diffusion together of II and BH. Since this reaction should be much slower than a diffusion-controlled reaction, this pathway for formation of phthalide can be excluded.

Formation of II *via* cyclization of $\mathbf{1}^-$ and subsequent conversion of II to products *via* IV (eq 10) can be ruled out as a mechanism for the base-catalyzed reaction. In this mechanism, proton transfer is never concerted with the breaking or making of a covalent bond to carbon, so that it is inconsistent with the observation $0 < \beta < 1$ at high pH values.

(14) M. Eigen, *Angew. Chem., Int. Ed. Engl.*, **3**, 1 (1964).
(15) R. B. Barnett and W. P. Jencks, *J. Amer. Chem. Soc.*, **91**, 2358 (1969).
(16) R. K. Chaturvedi and G. L. Schmir, *ibid.*, **91**, 737 (1969).

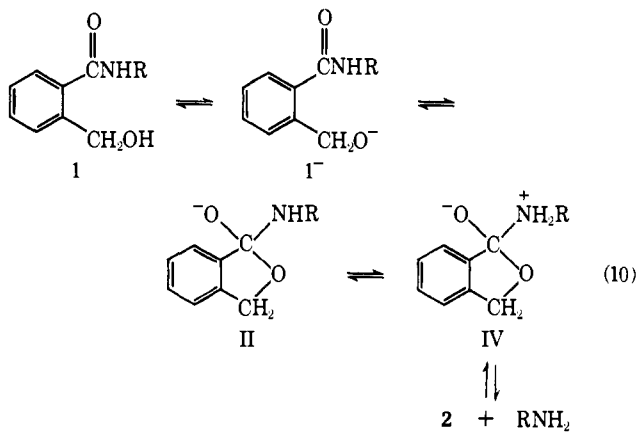

(10)

Dependence of K_1 on Buffer Concentration. In the scheme depicted in eq 8, both conversions of I to II and IV are rate determining for the base-catalyzed reaction, when $\beta = 1$. The maximum value of k_{-2} and k_3 is the rate constant for a diffusion-controlled reaction, k_d. The β value of unity demands that $k_{-2} = k_d$ and $k_3 > k_{-2}$, if conversion of I to II is rate limiting. If conversion of II to IV is rate limiting, $k_3 = k_d$ and $k_{-2} > k_3$. Since neither of these conditions can be satisfied, one must assume k_2 and $k_3 = k_d$ and both steps are rate determining when $\beta = 1$. The reaction pathway depicted in eq 8 leads to eq 11 which describes the dependence of K_1 on the concentration of acid $[BH_i]$ and base $[B_i]$. (Equations 11–15 appear in Chart I.) $K_{I,II}$, $K_{III,I}$, and K_{BHi} are the acid dissociation constants of I, III, and the acidic form of catalyst, i. K_I is the equilibrium constant for formation of I from **1**.

Below pH 6–8, the slope (K_{1B_i}) of a linear plot of K_1 *vs.* total buffer concentration at a constant buffer ratio is a linear function of the fraction of basic component in the buffer (f), and the catalytic efficiency of a base is described by the Brønsted equation with $\beta = 1$. These results are taken to mean that below pH 6–8, $\Sigma(k_{3BHi}[Bi]/K_{BHi})/\Sigma(k_{-2BHi}[Bi]/K_{BHi})$ = a constant ~ 1 and $\Sigma k_{1Bi}[Bi] + \Sigma k_{1BHi}'[BHi] \gg K_I K_{I,II}\Sigma(k_{3BHi}[Bi]/K_{BHi}) + (K_I/K_{III,I})\Sigma k_{5Bi}K_{BHi}[BHi]$.

Evidence for a Change in Rate-Controlling Step for Lactonization of 1a and 1b. The slopes of linear plots (K_{1B_i}) for imidazole-catalyzed lactonization of **1b** and the carbonate-catalyzed lactonization of **1a** are not linear functions of f (Figure 3). This result can be interpreted in terms of a change in rate-determining step as f is increased.

The linear dependence of K_1 on the total buffer concentration, [Bt] ([Bt] = [B] + [BH]), at a constant buffer ratio indicates that catalysis by species other than the acidic and basic forms of the buffer (*e.g.*, OH^-, H_3O^+, and H_2O) does not significantly effect values of the two terms

$$\Sigma(k_{3BHi}[Bi]/K_{BHi})/\Sigma(k_{-2BHi}[Bi]/K_{BHi})$$

and

$$\frac{1}{\Sigma k_{1Bi}[Bi] + \Sigma k_{1BHi}'[BHi]} \times \left[\frac{K_I K_{I,II}\,\Sigma(k_{3BHi}[Bi]/K_{BHi})}{1 + \Sigma(k_{3BHi}[Bi]/K_{BHi})/\Sigma(k_{-2BHi}[Bi]/K_{BHi})} + \frac{K_I}{K_{III,I}}\Sigma k_{5Bi}K_{BHi}[BHi]\right]$$

Chart I

$$K_1 = \frac{\dfrac{K_I K_{I,II}\Sigma(k_{3BHi}[Bi]/K_{BHi})}{1 + [\Sigma(k_{3BHi}[Bi]/K_{BHi})/\Sigma(k_{-2BHi}[Bi]/K_{BHi})]} + \dfrac{K_I}{K_{III,I}}\Sigma k_{5Bi}K_{Bi}[BHi]}{1 + \dfrac{1}{\Sigma k_{1Bi}[Bi] + \Sigma k_{1BHi}'[BHi]}\left[\dfrac{K_I K_{I,II}\Sigma(k_{3BHi}[Bi]/K_{BHi})}{1 + \Sigma(k_{3BHi}[Bi]/K_{BHi})/\Sigma(k_{-2BHi}[Bi]/K_{BHi})} + \dfrac{K_I}{K_{III,I}}\Sigma k_{5Bi}K_{BHi}[BHi]\right]} \quad (11)$$

$$K_{1B_t} = \frac{\left[\dfrac{K_I K_{I,II}k_{3BH}}{K_{BH}}\dfrac{f}{1 + (k_{3BH}/k_{-2BH})} + \dfrac{K_I k_{5B}K_{BH}(1-f)}{K_{III,I}}\right]}{1 + \dfrac{1}{k_{1B}f + k_{1BH}'(1-f)}\left[\dfrac{K_I K_{I,II}k_{3BH}}{K_{BH}}\dfrac{f}{1 + (k_{3BH}/k_{-2BH})} + \dfrac{K_I k_{5B}K_{BH}(1-f)}{K_{III,I}}\right]} \quad (12)$$

$$K_{1B_t} = \frac{\dfrac{K_I K_{I,II}k_{3HCO_3}f}{[1 + (k_{3HCO_3}/k_{-2HCO_3})]K_{HCO_3}}}{1 + \dfrac{1}{k_{1CO_3}f + k_{1HCO_3}'(1-f)}\left[\dfrac{K_I K_{I,II}k_{3HCO_3}f}{[1 + (k_{3HCO_3}/k_{-2HCO_3})]K_{HCO_3}}\right]} \quad (13)$$

$$K_{1_0} = \frac{\dfrac{K_I K_{I,II}[(k_{3H_2O}[OH^-]/K_{H_2O}) + (k_{3H_3O}[H_2O]/K_{H_3O})]}{1 + \dfrac{(k_{3H_2O}[OH^-]/K_{H_2O}) + (k_{3H_3O}[H_2O]/K_{H_3O})}{(k_{-2H_2O}[OH^-]/K_{H_2O} + (k_{-2H_3O}[H_2O]/K_{H_3O})}} + \dfrac{K_I}{K_{III,I}}(k_{5H_2O}K_{H_3O}[H_3O^+] + k_{5OH}K_{H_2O}[H_2O])}{1 + \dfrac{1}{(k_{1H_2O} + k_{1H_2O}')[H_2O] + k_{1OH}[OH^-] + k_{1H_3O}'[H_3O^+]} \times \left[\dfrac{K_I K_{I,II}[(k_{3H_2O}[OH^-]/K_{H_2O}) + (k_{3H_3O}[H_2O]/K_{H_3O})}{1 + \dfrac{(k_{3H_2O}[OH^-]/K_{H_2O}) + (k_{3H_3O}[H_2O]/K_{H_3O})}{k_{-2H_2O}[OH^-]/K_{H_2O} + (k_{-2H_3O}[H_2O]/K_{H_3O})}} + \dfrac{K_I}{K_{III,I}}(k_{5H_2O}K_{H_3O}[H_3O^+] + k_{5OH}K_{H_2O}[H_2O])\right]} \quad (14)$$

$$K_{1_0} = \frac{(K_1 K_{I,II}k_{3H_2O}[OH^-]/K_{H_2O}) + (K_1 K_{H_3O}k_{5H_2O}[H_3O^+]/K_{III,I}) + \left[\dfrac{K_{H_2O}k_{5OH}}{K_{III,I}} + k_{7H_2O}[H_2O]\right]K_I[H_2O]}{1 + \left[\dfrac{(K_I K_{I,II}k_{3H_2O}[OH^-]/K_{H_2O}) + (K_I K_{H_3O}k_{5H_2O}[H_3O^+]/K_{III,I}) + \left[\dfrac{K_{H_2O}k_{5OH}}{K_{III,I}} + k_{7H_2O}[H_2O]\right]K_I[H_2O]}{[k_{1H_2O} + k_{1H_2O}'][H_2O] + k_{1OH}[OH^-] + k_{1H_3O}'[H_3O^+]}\right]} \quad (15)$$

when the values of these terms are close to unity (*i.e.*, when both formation and decomposition of I are rate determining). The slope (K_{1B_i}) of the linear plots of K_1 *vs.* total buffer concentration (at a constant buffer ratio) is related to the fraction of the basic component in the buffer (f) by eq 12, provided neither component of the buffer is amphoteric.

Assuming that conversion of **1** to I becomes rate determining as f is increased, the dependence of K_{1B_i} on f leads to values of 4.0×10^{-3}, 0.18×10^{-3}, 4.9×10^{-3}, and 3.4×10^{-2} min^{-1} M^{-1} for $K_I K_{I,II} k_{3IMH}/K_{IMH}[1 + (k_{3IMH}/k_{-2IMH})]$, $K_I k_{5IM} K_{IMH}/K_{III,I}$, k_{1IM}, and k_{1IMH}', respectively for the imidazole-catalyzed lactonization of **1b** at 60°.

The dependence of K_{1B_i} on f for lactonization of amide **1a** at 40° in HCO_3^-–CO_3^{2-} buffers with $0.1 < f < 0.9$ was represented in terms of eq 13.

Values of 0.85, 0.2, and 0.25 min^{-1} M^{-1} were obtained for $K_I K_{I,II} k_{3HCO_3}/K_{HCO_3}[1 + (k_{3HCO_3}/k_{-2HCO_3})]$, k_{1CO_3}, and k_{1HCO_3}', respectively, from the dependence of K_{1B_i} on f for the carbonate-catalyzed lactonization of amide **1a** at 40°. Interpretation of the dependence of K_{B_i} on f in terms of eq 13 involves the assumption

$$\frac{K_I K_{I,II} k_{3HCO_3} f}{K_{HCO_3}[1 + (k_{3HCO_3}/k_{-2HCO_3})]} > \frac{K_I K_{HCO_3} k_{5CO_3}(1 - f)}{K_{III,I}} + \frac{K_I K_{I,II} k_{3H_2CO_3}(1 - f)}{K_{H_2CO_3}[1 + (k_{3H_2CO_3}/k_{-2H_2CO_3})]}$$

when $0.1 < f < 0.9$. This assumption is reasonable, since $K_I K_{HCO_3} k_{5CO_3}/K_{III,I}$ should be smaller than $K_I K_{HAC} k_{5AC}/K_{III,I} = 7.5 \times 10^{-4}$ min^{-1} M^{-1}, and $K_I K_{I,II} k_{3H_2CO_3}/K_{H_2CO_3}[1 + (k_{3H_2CO_3}/k_{-2H_2CO_3})]$ should be smaller than $K_I K_{I,II} k_{3HAC}/K_{HAC}[1 + (k_{3HAC}/k_{-2HAC})] = 6.5 \times 10^{-5}$ min^{-1} M^{-1}, whereas the dependence of K_{1B_i} on f (eq 13) gives a value of 0.85 min^{-1} M^{-1} for $K_I K_{I,II} \cdot k_{3HCO_3}/K_{HCO_3}[1 + (k_{3HCO_3}/k_{-2HCO_3})]$.

The upward curvature of plots of K_{1B_i} *vs.* f observed for lactonization of **1b** in $H_2PO_4^-$–HPO_4^{2-} buffers is difficult to interpret quantitatively (Figure 3). Added to the possibility of a change in rate-determining step occurring in the range $0.1 < f < 0.9$, is the possibility of a contribution to K_{1B_i} from PO_4^{3-}-catalyzed lactonization. The upward curvature of the plot of K_{1B_i} *vs.* f for lactonization of **1a** in $H_2PO_4^-$–HPO_4^{2-} buffers is probably primarily due to PO_4^{3-}-catalyzed lactonization rather than a change in rate-determining step. The plot of K_{1B_i} *vs.* f for imidazole-catalyzed lactonization of **1a** is linear. Imidazole is a stronger base than HPO_4^{2-} at 40°, so that a change in rate-determining step would not be expected in $H_2PO_4^{2-}$–HPO_4^{2-} buffers, when it is not observed in imidazole buffers. For the $H_2PO_4^-$–HPO_4^{2-} buffers, $f < 0.9$, so that $[PO_4^{3-}] \ll [H_2PO_4^-]$ or $[HPO_4^{2-}]$. Therefore, eq 16 should describe

$$K_{1B_i} = fK_{1HPO_4} + (1 - f)K_{1H_2PO_4} + \frac{K_{HPO_4}}{[H^+]} fK_{1PO_4} \quad (16)$$

the dependence of K_{1B_i} on f for catalysis of lactonization of **1a** by $H_2PO_4^-$–HPO_4^{2-} buffers. K_{1HPO_4}, $K_{1H_2PO_4}$, and K_{1PO_4} are the apparent second-order rate constants for catalysis of lactonization by HPO_4^{2-}, $H_2PO_4^-$, and PO_4^{3-}, respectively. K_{HPO_4} is the acid dissociation constant of HPO_4^{2-}. Fitting the dependence of K_{1B_i} (for lactonization of **1a** at 40°) on f to eq 16 leads to values of 3.75×10^{-3}, 0.8×10^{-3}, and 11 min^{-1} M^{-1} for K_{1HPO_4}, $K_{1H_2PO_4}$, and K_{1PO_4}, respectively. Significantly, the value of K_{1PO_4} (11 min^{-1} M^{-1}) is more than 10 times the apparent second-order rate constant for PO_4^{3-}-catalyzed lactonization of **1a** obtained in HPO_4^{2-}–PO_4^{3-} buffers. This result further supports the conclusion that the rate-determining step in lactonization of amide **1a** changes at pH ~8. The two values obtained for K_{1PO_4} reflect PO_4^{3-} catalysis of different steps. In terms of eq 12, $K_I K_{I,II} k_{3HPO_4}/K_{HPO_4}[1 + (k_{3HPO_4}/k_{-2HPO_4})] = 11$ min^{-1} M^{-1} and $k_{1PO_4} = 0.8$ min^{-1} M^{-1}.

Further Evidence for a Change in Rate-Controlling Step pH–Rate Profile of 1a. The pronounced breaks in the pH–rate profile for lactonization of **1a** are another indication that lactonization of **1a** involves a multistep reaction with a change in rate-determining step occurring at pH 8–9. Equation 14 describes the dependence of K_1 on $[H_3O^+]$ at zero buffer concentration in terms of the reaction scheme depicted in eq 9.

Below pH 8.5, decomposition of I to products should be rate determining ($\beta = 1$ or 0 for base-catalyzed lactonization). In the pH range 7–8.5, hydroxide ion makes a major contribution to the rate, *i.e.*, $k_{3H_2O}[OH^-]/K_{H_3O} > k_{3H_3O}[H_2O]/K_{H_3O}$ or $k_{-2H_2O}[OH^-]/K_{H_2O} > k_{-2H_2O}[H_2O]/K_{H_3O}$. Hydronium ion should be a stronger acid than $-NH_2^+R$ in IV or $-OH$ in I, so that the reactions

$$II + H_3O^+ \xrightarrow{k_{3H_3O}} IV + H_2O$$

and

$$II + H_3O^+ \xrightarrow{k_{-2H_3O}} I + H_2O$$

are thermodynamically favored, and thus, k_{3H_3O} and $k_{-2H_3O} \sim k_d$. Since hydroxide ion should be a stronger base than $-NHR$ in II, $k_{-3OH} \sim k_d$ and $k_{3H_2O} = k_d K_{H_2O}/K_{IV,II}$. Assuming the OH group in I is a weaker acid than the NH_2^+R group in IV (*i.e.*, $K_{I,II} < K_{IV,II}$) it follows that $k_{3H_2O} < k_{-2H_3O}$. Thus, the second-order rate constant for hydroxide ion catalyzed lactonization of **1a** between pH 7 and 8.5 is $K_I K_{I,II} k_{3H_2O}/K_{H_2O}$.

Between pH 4.5 and 6.5, the observed rate constant for lactonization of **1a** is independent of $[OH^-]$ and $[H_3O^+]$ and a water-catalyzed lactonization appears to make the major contribution to the rate. If formation of product through water-catalyzed decomposition of III were negligible, the rate constant for water-catalyzed lactonization would be between $K_I K_{I,II} k_{3H_3O}/K_{H_3O}$ and $K_I K_{I,II} k_{3H_3O}/2K_{H_3O}$, depending on whether $k_{-2H_2O} \cdot [OH^-]/K_{H_2O}$ were greater or smaller than $k_{-2H_3O}[H_2O]/K_{H_3O}$ between pH 4.5 and 6.5 ($k_{3H_3O} \sim k_{-2H_3O}$ and $k_{-2H_2O} > k_{3H_2O}$). A rough estimate for $K_I K_{I,II} k_{3H_3O}/2K_{H_3O}$ of 3×10^{-11} min^{-1} M^{-1} can be obtained by extrapolating the Brønsted plot obtained for acetate, succinate, HPO_4^{2-}, and imidazole-catalyzed lactonization of **1a** to the pK_a of H_3O^+. The possibility that the observed rate constant for the water-catalyzed reaction of 8.2×10^{-7} min^{-1} M^{-1} is primarily due to reaction of water with I to form II or reaction of hydronium ion with II to form IV seems unlikely in light of the observed deviation of over four orders of magnitude from the Brønsted relationship. The water-catalyzed reaction might be attributed primarily to catalysis by water (acting as a base) of the elimination of amine from III. At 60°, water is roughly 20 times more efficient a catalyst than predicted by the Brønsted relationship for acid catalysis of the lactonization of amide **1a** (Figure 5).

Perhaps decomposition of I directly to products *via* a cyclic transition state (*e.g.*, VI) is responsible for the enhanced catalytic efficiency of water.

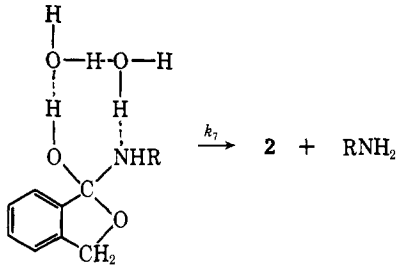

VI

Structure VII represents possible transition states for the acid- and base-catalyzed transition **1** → I. In VII,

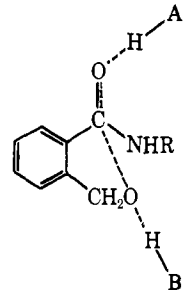

VII

In light of the considerations discussed, the dependence of K_{1_0} on $[H_3O^+]$ for lactonization of **1a** was interpreted in terms of eq 15.

Fitting the observed dependence of K_{1_0} on $[H_3O^+]$ for lactonization of **1a** at 40° to eq 15 leads to values of 150, 0.517, 8.2×10^{-7}, 3.8, 4.5×10^{-5} min^{-1} M^{-1} for $K_I K_{I,II} k_{3H_2O}/K_{H_2O}$, $K_I K_{H_3O} k_{5H_2O}/K_{III,I}$, $[(K_{H_2O} k_{5OH}/K_{III,I}) + k_{7H_2O}[H_2O]]K_I$, k_{1OH}, and $(k_{1H_2O} + k_{1H_2O}')$, respectively (Figure 4). The value of $k_{1H_3O}'[H_3O^+]$ was assumed to be small relative to $(k_{1H_2O} + k_{1H_2O}')[H_2O] + k_{1OH}[OH^-]$ at the low hydronium ion concentrations where formation of I is rate controlling.

Brønsted Relationships. A Brønsted plot for base-catalyzed lactonization of **1a** under conditions where decomposition of I (*via* II and IV) to products is rate determining appears in Figure 5. The dependence of the catalytic efficiency of Bi on K_{BHi} is exactly what one would expect for diffusion-controlled proton transfer. Eigen[14] demonstrated that the rate constant for proton transfer in the thermodynamically favored direction is equal to the rate constant (k_d) for a diffusion-controlled reaction. Therefore, when $K_{BHi} > K_{IV,II} > K_{I,II}$, $k_{3BHi} = k_{-2BHi} = k_d$ and $K_{1_b} = K_I K_{I,II} k_d/2K_{HBi}$; and when $K_{BHi} < K_{IV,II} > K_{I,II}$, $k_{3BHi} = K_{BHi} k_d/K_{IV,II} < k_{-2BHi}$ and $K_{1_b} = K_I K_{I,II} k_d/K_{IV,II}$. Thus the Brønsted β value will change from unity to zero as the acid dissociation constant of the catalyst becomes less than the acid dissociation constant of intermediate IV. Because of special proton transport mechanisms available to hydrated hydroxide ions and protons in water, k_d increases somewhat more than an order of magnitude when one of the reactants in a diffusion-controlled proton transfer is hydroxide or hydronium ion. For example, the rate constant for diffusion-controlled proton transfer from ammonium ion to hydroxide ion is 21.5 times greater than the rate constant for diffusion-controlled proton transfer from ammonium ion to the conjugate base of glucose.[14] Thus, the ~20-fold positive deviation observed for hydroxide ion catalyzed lactonization (when decomposition of II is rate determining, Figure 5), is consistent with the mechanism in which diffusion-controlled proton transfer limits the rate of decomposition of intermediate II to products.

A Brønsted plot for base-catalyzed lactonization of **1a** under conditions where formation of I is rate determining yields a value of 0.2 for β (Figure 6). Acids also catalyze this step (*e.g.*, the apparent second-order rate constant (k_{1IMH}') for catalysis of the transition **1b** → I by imidazolium ion is 3.4×10^{-2} min^{-1} M^{-1} at 60°). A or B is a proton acceptor other than H_2O or OH^-. Acid catalysis is observed when the remaining group (B or A) is H_2O and base catalysis is observed when the remaining group is OH^-.

The lower rate constants of base- and acid-catalyzed attack observed for **1b** in comparison to **1a** are not unexpected. The bulky, electron-donating $ArCH_2$ group would be expected to hinder cyclization of **1** to tetrahedral intermediate I by decreasing the positive charge density on the carbonyl carbon and sterically blocking the transition from trigonal carbon to tetrahedral carbon. Assuming $K_{I,II}$ for amides **1a** and **1b** are roughly equal, K_I for amide **1b** is roughly one-tenth K_I for amide **1a** (as estimated from the ratio of values of $K_I K_{I,II} k_d/2K_{IMH}$ determined for the imidazole-catalyzed lactonization of amides **1a** and **1b**).

Comparison of Imidazole-Catalyzed Lactonization of 1a with Formation of Acylchymotrypsins. The imidazole-catalyzed lactonization of **1a** can be considered as a reasonable model for the acylation of chymotrypsin by its best low molecular weight amide substrates.

Assuming that the local concentration of an imidazole group around the "active serine" residue of a serine proteinase is 20 *M*,[17] a rate constant of 9.0×10^{-2} min^{-1} would be expected for formation of an acyl-enzyme from an enzyme–substrate complex in which the relative orientation of the hydroxyl and amido groups was similar to that existing in model compound **1a**. This value is only 23–280 times less than the rate constant observed for formation of acylchymotrypsin intermediates from the best known low molecular weight amide substrates for chymotrypsin. At 25°, pH 7.9, the rate constants for the acylation of chymotrypsin by acetyl-L-tryptophanamide, acetyl-L-tyrosinamide, and isonicotinyl-L-tyrosinamide are 2.1, 9.5, and 25 min^{-1}, respectively.[18] The dependence of the rate constant for acylation of chymotrypsin on the nature of the amide substrate is probably a consequence of the spatial relationship between the α-carbonyl carbon atom of the substrate and the hydroxyl group of Ser-195 in the chymotrypsin–substrate complex. By analogy, it should be possible to further account for rates of acylation of chymotrypsin by adjusting the relative orienta-

(17) (a) For discussion of changes in the values of rate constants on going from a bimolecular reaction to a unimolecular reaction with no change in mechanism see ref 17b–c; (b) D. E. Koshland, Jr., *J. Theoret. Biol.*, **2**, 75 (1962); (c) T. C. Bruice and S. J. Benkovic, *J. Amer. Chem. Soc.*, **86**, 418 (1964), and references cited therein.

(18) R. J. Foster and C. Niemann, *ibid.*, 77, 1886 (1955).

tion of amido and hydroxyl groups in model compounds so that the positions of these groups in the ground state more closely resemble their positions in the transition state for lactonization.

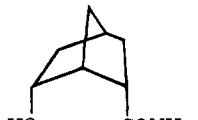

5

Perhaps the hydroxyamide **5** will be more susceptible than **1a** to imidazole-catalyzed lactonization. The parent acid of **5** has been reported to lactonize $\sim 3 \times 10^4$ times faster than hydroxymethylbenzoic acid.[19]

(19) D. R. Storm and D. E. Koshland, Jr., *Proc. Nat. Acad. Sci. U.S.*, 66, 445 (1970).

Polyene Macrolide Antibiotic Amphotericin B.[1] Crystal Structure of the *N*-Iodoacetyl Derivative

Paolo Ganis,*[2,3] Gustavo Avitabile,[2,4] Witold Mechlinski,*[5] and Carl P. Schaffner[5]

Contribution from the Polymer Research Institute, Polytechnic Institute of Brooklyn, Brooklyn, New York 11201, and the Institute of Microbiology, Rutgers University, The State University of New Jersey, New Brunswick, New Jersey 08903.
Received October 12, 1970

Abstract: The *N*-iodoacetyl derivative of the important antifungal polyene macrolide antibiotic amphotericin B was found to be biologically active and was used as a heavy atom derivative of the antibiotic for X-ray single-crystal analysis. Monoclinic crystals of the *N*-iodoacetylamphotericin B tritetrahydrofuran monohydrate, $C_{49}H_{74}O_{18}NI \cdot 3C_4H_8O \cdot H_2O$, were grown from tetrahydrofuran solution. The unit cell parameters are: $a = 21.28$, $b = 8.78$, $c = 18.69$ Å, $\beta = 103° 58'$, $V = 3387$ Å^3, $Z = 2$, $D_m = 1.33$, $D_c = 1.30$, space group $P2_1$. Data were collected for 3702 reflections including 2658 nonzero ones with a Picker automated diffractometer. The structure was solved by the Patterson method to the reliability R factor of 0.137. The following features of the molecule of the antibiotic were indicated for the first time: the presence of a ketalic six-membered ring included in the macrolactone ring, the locations of all the hydroxylic groups, and the position of the β-glycosidically bound mycosamine moiety in the form of a pyranoside. The crystal structure is described in terms of intermolecular hydrogen bondings. The function of the solvent molecules in the crystal is also explained.

N-Iodoacetylamphotericin B is a biologically active heavy atom derivative of one of the most important polyene macrolide antibiotics, amphotericin B (review by Oroshnik and Mebane[6]). Antibiotics of this group of natural products have in common a very pronounced activity against yeast and fungi. They found medical use in the treatment of systemic mycotic infections caused by *Candida albicans*, *Cryptococcus neoformans*, and other pathogenic fungi. Very recently, Gordon and Schaffner[7,8] discovered the effect of these antibiotics on prostatic hypertrophy and hypercholesterolemia in animals.

Because of the difficulties in purification, the very unstable chemical character, and large molecular weight (*ca.* 700–1300) the chemical investigation of the polyenic macrolide antibiotics is a complicated task, and only a few partial structures have been described out of the *ca.* 80 antibiotics reported in the literature. No total structure as yet has been described. The polyenic macrolide antibiotics feature a large number of asymmetric centers in the molecule and also may undergo a cis–trans transformation of the chromophore. The elucidation of the full chemical and stereochemical structure of these molecules is very important for a better understanding of the relationship between similar members of this antibiotic family and their behavior in chemical and biological studies. It is very likely that some polyenic antibiotics have identical chemical structures but are stereochemical isomers.

Amphotericin B, described in 1956 by Vandeputte, Wachtel, and Stiller,[9] is produced by *Streptomyces nodosus*. The chemical structure of this antibiotic was investigated since 1957.[10–15] The results can be summarized by the partial chemical structure of

(1) The chemical structure and absolute configuration of amphotericin B: W. Mechlinski, C. P. Schaffner, P. Ganis, and G. Avitabile, *Tetrahedron Lett.*, 3873 (1970).
(2) Polytechnic Institute of Brooklyn.
(3) On sabbatical leave from Universita' di Napoli, Istituto Chimico, Napoli, Italy.
(4) Postdoctoral Fellow on leave from Universita' di Napoli, Istituto Chimico.
(5) Institute of Microbiology.
(6) W. Oroshnik and A. D. Mebane, *Fortschr. Chem. Org. Naturst.*, 21, 17 (1963).
(7) H. W. Gordon and C. P. Schaffner, *Proc. Nat. Acad. Sci. U. S.*, 60, 1201 (1968).
(8) C. P. Schaffner and H. W. Gordon, *ibid.*, 61, 36 (1968).
(9) J. Vandeputte, J. L. Wachtel, and E. T. Stiller, *Antibiot. Annu.*, *1955–1956*, 579 (1956).
(10) J. D. Dutcher, M. B. Young, J. H. Sherman, W. Hibbits, and D. R. Walters, *ibid.*, *1956–1957*, 866 (1957).
(11) E. Borowski, W. Mechlinski, L. Falkowski, T. Ziminski, and J. D. Dutcher, *Tetrahedron Lett.*, 473 (1963).
(12) L. Falkowski, T. Ziminski, W. Mechlinski, and E. Borowski, *Rocz. Chem.*, 39, 225 (1965).
(13) E. Borowski, W. Mechlinski, L. Falkowski, T. Ziminski, and J. D. Dutcher, *ibid.*, 39, 400 (1965).
(14) W. Mechlinski, T. Ziminski, L. Falkowski, and E. Borowski, *ibid.*, 39, 497 (1965).
(15) E. Borowski, W. Mechlinski, L. Falkowski, T. Ziminski, and J. D. Dutcher, *ibid.*, 39, 1933 (1965).